ACADEMIA MATERIALS SCIENCE

Research Article
Published: 2023-12-08
https://doi.org/10.20935/AcadMatSci6142

Sol–gel synthesis of TiO_2 doped with chromium: photocatalytic degradation of tartrazine

Ana E. Cardozo[1], Elsa M. Farfán Torres[2], Graciela V. Morales[1,*], Edgardo L. Sham[1]

Academic Editor(s): Manickam Minakshi and Raul D.S.G. Campilho

Abstract

Photocatalysis is an advanced oxidation method that allows the removal of aqueous pollutants of different origins. However, its application on an industrial scale is limited due to the requirement of excitation sources in UV frequency. For this reason, it is important to develop photocatalytic materials capable of working under visible radiation in photodegradation processes. This study analyzes the synthesis of TiO_2 nanoparticles, using a new sol–gel route in a nonpolar dissolvent and its modification by doping with different chromium VI ion concentrations: 0.5, 1.0, and 1.5% w/w. A novel modification of this synthesis technique is reported, in which a nonpolar solvent, C_6H_{12}, is used to control the hydrolysis reactions of the titania precursor. Similarly, the use of ammonium chromate, $(NH4)_2CrO_4$, introduced by means of the impregnation-by-moisture-incipient technique, is proposed as a precursor of Cr dispersed in the TiO_2 network, together with the study of the influence of chromium content on the photocatalytic activity of solids. The solids obtained by this technique were heat-treated at 400°C and characterized by Fourier Transform Infrared Spectroscopy (FTIR), Raman Spectroscopy, Diffuse Reflectance Spectroscopy, X-Ray Diffraction (XRD), N_2 Sorptometry, and Zeta Potential. Doping of titania with chromium stabilizes the crystalline phases of anatase and brookite. In addition, the introduction of chromium (VI) ions tends to reduce the average size of the particles, increasing the specific surface area and favoring the development of a mesoporous structure. It also decreases the forbidden band (E_g) and increases the absorption of radiation in the visible light range.

Keywords: *TiO_2, Cr (VI), doping, photocatalysis, tartrazine, sol–gel*

Citation: Cardozo AE, Farfán Torres EM, Morales GV, Sham EL. Sol–gel synthesis of TiO2 doped with chromium: photocatalytic degradation of tartrazine. *Academia Materials Science* 2023;1. https://doi.org/10.20935/AcadMatSci6142

1. Introduction

Heterogenous photocatalysis is one of the technologies that composes the advanced processes of oxidation, where a semiconductor generates an electron–hole pair because of the transition of an electron from the valence band to the conduction band.

If these charge carriers succeed in being available on the semiconductor surface, then the holes can produce *OH radicals, which are highly reactive due to the oxidation of OH^- or H_2O. On the other hand, electrons can catch molecular oxygen to form a superoxide radical anion O_2^{*-}, which is another highly reactive kind. One of the most studied semiconductors in heterogeneous photocatalysis is TiO_2, which is frequently used in photocatalytic reactors for water remediation [1], air purifiers built with photocatalytic membranes, anti-fog glasses covered by a thin layer of photocatalyst, construction materials that contain photocatalysts in their structure, used in air remediation [2, 3], among other applications.

In addition to numerous other advantages, TiO_2 proves to be chemically and biologically inert and stable against chemical and photochemical corrosion. However, it is worth mentioning some weaknesses: it presents a rapid recombination between electrons and photogenerated holes, which results in a low use of irradiated light. Furthermore, this semiconductor is only photoactive under an ultraviolet light source due to the value of its band gap.

Much research has been done on modifying the physicochemical properties of TiO_2 to shift its absorption threshold to the visible region and separate the photoinduced charges [4, 5]. This is possible by coupling it to organic or inorganic dyes [6, 7], or by modifying its surface with other semiconductors [8], doping it with cations, anions, or metals [9], particularly with transition elements such as Ag [10], Au [11], Fe [12], and Cr [13, 14], among others.

It is known that TiO_2 photocatalytic reactivity can be extended to the range of visible light by means of doping. Doping ions from transition metals can replace Ti^{4+} ions in the titania lattice, thus being able to cause band gap decrease, which enables absorption under visible radiation. Doping ions can also act as capture

[1]Research Institute for Chemical Industry INIQUI-CONICET, Faculty of Engineering, National University of Salta, CIUNSa, 4400 Salta, Argentina.
[2]Research Institute for Chemical Industry INIQUI-CONICET, Faculty of Exact Sciences, National University of Salta, CIUNSa, 4400 Salta, Argentina.
*email: gmorales@unsa.edu.ar

centers or electron traps that can change the average lifespan of the generated charge carriers, thus decreasing their recombination [15]. Chromium is ranked as one of the most promising dopants for enhancing photo responsiveness in the wavelength range of visible radiation, as demonstrated in several studies related to the photodegradation of organic dyes in water [13, 14]. Chromium can modify the optical, electrical, and structural properties of titanium dioxide due to its ability to alter the rate of recombination of charge carriers. This doping has different oxidation states. Thus, the obtained product is expected to produce multiple mid-gap energy levels in the band structure that modify the electronic properties of TiO_2 [16, 17]. **Table 1** shows comparative studies of materials doped with chromium versus materials doped with iron and copper.

Table 1 • Comparative studies of materials doped with some other metals

Photocatalyst	Synthesis method	Light source	Contaminant	Removal efficiency	References
Cu-TiO_2	Solvothermal	Visible Light	Congo Red Methylene Blue	99%	Bibi et al. [18]
Fe-TiO_{2-x}	Via calcination method	Visible Light	Tetracycline	88.21% Catalyst amount 125 mg 73.93% pH = 11	Hou et al. [19]
TiO_2-Cr	Sol–gel	UV Light	Phenol	95%	López et al. [20]

In this study, the versatile sol–gel method is used as the titania synthesis method, since it provides a way of obtaining materials with different properties by controlling synthesis variables such as pH, temperature, or by adding surfactant materials and peptizers. In our case, an innovation was introduced in this synthesis method, using $C_{12}H_6$ as the reaction medium, which makes it possible to obtain a high dispersion of the hydrolysis agent. In this way, the hydrolysis and condensation reactions are controlled in a very simple and efficient way, allowing the architecture of the titania obtained to be controlled. Similarly, the use of ammonium chromate, $(NH_4)_2CrO_4$, introduced by means of the impregnation-by-moisture-incipient technique, is proposed as a precursor of Cr dispersed in the TiO_2 network, together with the study of the influence of chromium content, on the photocatalytic activity of solids.

2. Materials and methods

The following reactants were used for the preparation of solids: titanium isopropoxide (Aldrich 97%) as the precursor of TiO_2, *n*-isopropyl alcohol as the TIP dissolvent, cyclohexane (C_6H_{12}) as the hydrophobic medium, ammonium chromate $(NH_4)_2CrO_4$ (PA) as the chromium precursor, and bidistilled water.

2.1. Sol–gel synthesis of TiO_2

A specific volume of cyclohexane was poured into a beaker to which the aliquots of an alcoholic IPT solution and double-distilled water were added dropwise with vigorous stirring. Once the reactants were added, gel dispersion was kept stirring for 2 hours. Afterward, the resulting solid was dried in an oven at 70°C for 24 hours. The dry solid was ground in an agate mortar until a white homogeneous and finely divided powder was obtained, which is called TiO_2-CH.

2.2. Doping with chromium

An aqueous dissolution of ammonium chromate $(NH_4)_2CrO_4$ was used as the chromium source. Doping with Cr ions was performed by means of the impregnation-by-incipient-moisture technique. With this purpose, the point of incipient moisture of the dry solid to be impregnated was determined, thus yielding 0.8 mL/g.

Solids were doped with different percentages of chromium: 0.5%, 1.0%, and 1.5% Cr w/w, in order to verify that good photocatalytic results are obtained with small amounts of the dopant. The catalysts were named: 0.5Cr-TiO_2; 1.0Cr-TiO_2; and 1.5Cr-TiO_2. The impregnated solids were dried at 70°C for 24 hours.

Figure 1 shows a scheme of the sol–gel process followed by impregnation.

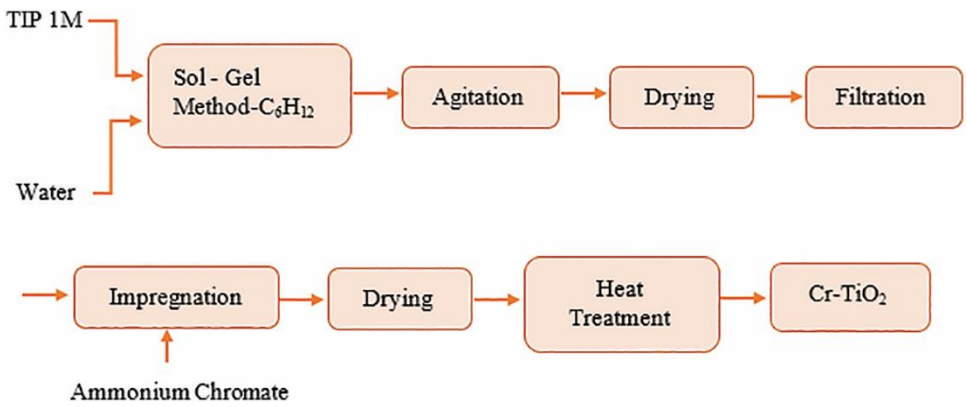

Figure 1 • Scheme of the sol–gel process followed by impregnation.

2.3. Characterization methods

Synthesized solids were calcined at 400°C, in static air, for 1 hour at a heating rate of 10°C/min. The calcination temperature was 400°C, since a better photocatalytic activity was obtained for the solids thermally treated at this temperature, compared to solids treated at 300 and 500°C.

Calcined solids were characterized by Infrared Spectroscopy (FTIR) and Raman Spectroscopy, by means of a Perkin Elmer FT-IRGX spectrophotometer equipped with a laser as the excitation source and KBr as the sample support medium for the FTIR analysis.

Diffuse reflectance measurements were carried out by using a UV-vis spectrophotometer equipped with an integration sphere with $BaSO_4$ as the reference, in analysis ranging from 190 to 800 nm. X-Ray Diffraction (XRD) studies were performed on a Rigaku diffractometer using CuKα radiation.

Zeta potential measurements were performed on a Z-Meter 3.0+ device. To this end, KNO_3 suspensions were prepared with 0.1 g/L sample concentration and an ionic power of 10^{-2} M. The graphs showing the variation of zeta potential as a function of pH were drawn. The pH of the medium was modified by adding solutions of HNO_3 or KOH, with concentrations 0.1 and 0.01 M, respectively, keeping the dispersion in contact for as long as necessary to reach equilibrium.

The textural characterization of solids was determined by adsorption–desorption isotherms obtained in a Micromeritics ASAP 2020 device at 77 K. The samples were previously degassed at 150°C. From the adsorption isotherms, the specific superficial area was calculated by using the Brunauer, Emmet, and Teller (BET) method. Micropore volume (Vμp) and pore total volume (V_{TP}) were calculated by using the Gurvich method. Pore size distribution was determined with the aid of the Barret-Joyner-Halenda (BJH) method for the adsorption branch.

2.4. Photocatalytic tests

The photocatalytic reaction was carried out on a glass reactor with a capacity of 200 mL. The organic compound under study is an aqueous solution of artificial dye tartrazine with an initial concentration of 1.0×10^{-5} M. A catalyst concentration of 1.0 g/L was used in all photocatalytic tests. The photocatalyst was previously dispersed in darkness in the tartrazine solution and was kept under stirring for 30 minutes to reach adsorption–desorption equilibrium. Afterward, the photoreactor was irradiated with visible light.

Tartrazine degradation was monitored by sampling at 30-minute intervals, over a period of 3 hours. A direct lighting reactor formed by four dichroic LED lamps was used as the visible light source. The emission spectrum of the lamps being used was measured using a Newport OSM-400 UV and 400 UV/vis optical spectrometer.

3. Results and discussion

3.1. X-ray diffraction

XRD studies were performed by using the powder method, which enabled the identification of two TiO_2 crystalline phases: anatase and brookite, the former being predominant. In **Figure 2**, the diffractograms of TiO_2-CH and its derivatives doped with chromium are presented.

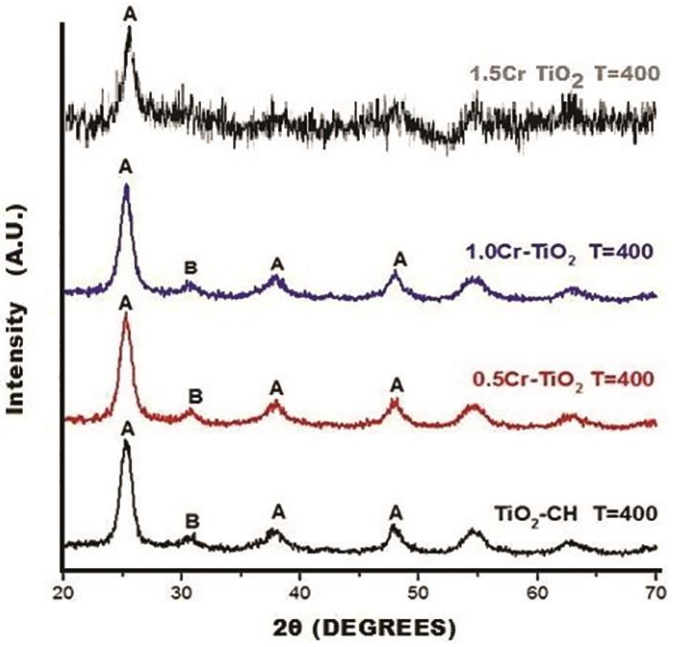

Figure 2 • XRD TiO_2-CH; 0.5Cr-TiO_2; 1.0Cr-TiO_2; 1.5Cr-TiO_2 calcined at 400°C. A (Anastase), B (Brookite).

Although there are no significant differences between these diffractograms, the 1.5Cr-TiO_2 photocatalyst shows a lower crystallinity. Complementing these studies with those of Raman spectroscopy, which are discussed later, we can infer that the incorporation of chromium ions stabilizes the anatase and brookite crystalline phases [20].

The fact that segregated Cr compounds are not detected in these diffractograms may be due to the fact that the concentration of the dopant (Cr) is so low that it cannot be detected by this technique [21]. However, it could also be indicative that chromium as a dopant in titania does not show a tendency to segregate and/or precipitate in different phases during the doping and heat treatment processes. Within the range of the thermal treatments used here, no diffraction lines related to the rutile TiO_2 phase were observed, neither in the pure nor in the doped samples.

Tables 2 and **3** show lattice parameters and crystal sizes for doped and undoped solids. The average size of crystals was determined by using the Scherrer equation:

$$D_{hkl} = \frac{5.3\lambda}{\beta(^\circ)\cos\theta} \quad (1)$$

where:

λ is the wavelength CuKα = 1.541874 Å.

β is the width of the peak at half height (FWHM).

These results show that there is a tendency for the mean crystal size to decrease with chromium doping for the predominant crystalline phase anatase. However, this decrease is insignificant, as are the changes in the values of unitary cell parameters, which are even less significant in the non-predominant phase. This fact would indicate that there is a real substitution of chromium ions in the anatase TiO_2 lattice [21].

Table 2 • Brookite lattice parameters and crystal size

Solids (calcined at 400°C)	Space group	Cell parameters (Å)	Cell volume (Å³)	Crystal size (Å)
TiO_2-CH	Pbca (61)	a = 9.184 b = 5.447 c = 5.145	257.38	57
0.5Cr-TiO_2	Pbca (61)	a = 9.184 b = 5.447 c = 5.145	257.38	62
1.0Cr-TiO_2	Pbca (61)	a = 9.191 b = 5.463 c = 5.157	258.94	55

Table 3 • Anatase lattice parameters and crystal size

Solids (calcined at 400°C)	Space group	Cell parameters (Å)	Cell volume (Å³)	Crystal size (Å)
TiO_2-CH	I41/amd (141)	a = b= 3.7892 c = 9.537	136.93	63
0.5Cr-TiO_2	I41/amd (141)	a = b = 3.73 c = 9.37	130.36	58
1.0Cr-TiO_2	I41/amd (141)	a = b = 3.7971 c = 9.579	138.11	57

3.2. Infrared spectroscopy

Through the FTIR study, it was possible to verify the presence of functional groups such as OH– groups. Hydroxyl groups are hole trappers produced because of the electronic excitation of incident radiation, which contributes to the improvement of photocatalytic activity.

The results of FTIR of solids are shown in **Figure 3**.

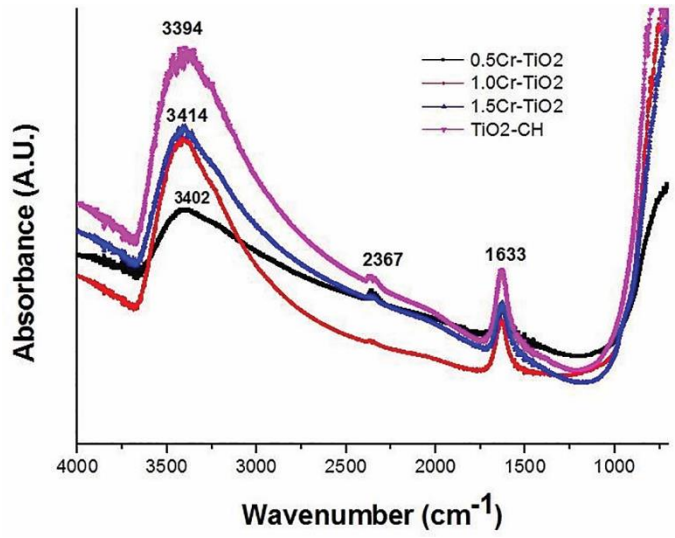

Figure 3 • FTIR spectra of undoped and Cr-doped TiO_2 (400°C).

A wide peak can be seen at approximately 3,400 cm^{-1} resulting from OH^- groups from the water molecules adsorbed at the surface of solids. A smaller peak was also detected at 1,633 cm^{-1} related to the bending vibration of OH at the surface. The peak at 2,367 cm^{-1} is related to residual organic groups. The relative intensity of these signals shows no significant variation with chromium content [13, 22].

3.3. Raman spectroscopy

Raman spectra of synthesized solids, doped and undoped are shown in **Figure 4**. Through these analyses, the phases detected by XRD were confirmed and can be used to determine the relative crystallinity of the Cr-doped TiO_2 materials.

Two TiO_2 polymorphs were detected: anatase majority phase and brookite minor phase, giving rise to well-defined bands around 400, 517, and 640 cm^{-1}, which agrees with what was observed in XRD for TiO_2-CH and Cr-TiO_2 with low chromium content, treated at 400°C. Including the superimposition of two fundamental peaks near 517 cm^{-1}, these four peaks correspond to the well-known fundamental vibrational modes of anatase TiO_2 with the symmetries of B_{1g}, A_{1g}, B_{1g}, and E_g, respectively, and B_{1g} and B_{2g} vibrational modes of brookite at 329 and 366 cm^{-1}, respectively [15].

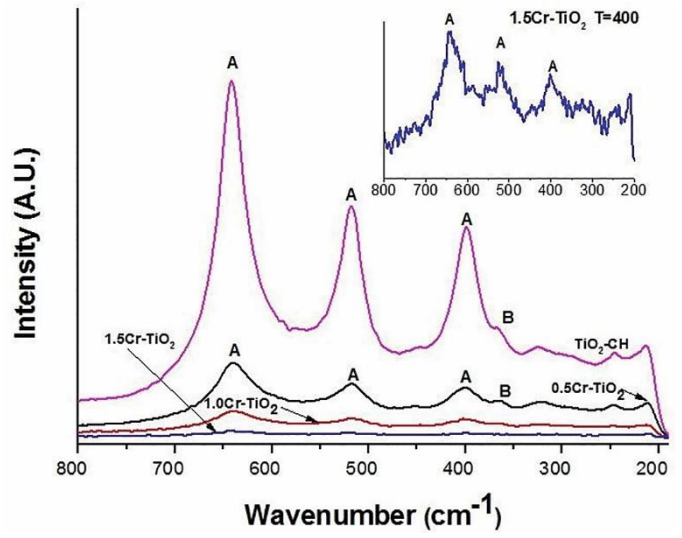

Figure 4 • Raman spectra of TiO_2 and Cr-doped TiO_2 (400°C). Amplification corresponds to 1.5Cr-TiO2. A (Anastase), B (Brookite).

It was observed that increasing the dopant concentration tends to slow down the crystallinity of the anatase and brookite phases. Likewise, the presence of crystalline phases corresponding to the dopant was not observed in the Raman spectra [23].

3.4. UV-Vis diffuse reflectance spectroscopy (DRS)

The study of optical properties of solids is important to analyze the response of photocatalysts under UV-Vis radiation. **Figure 5** shows the UV-Vis optical absorption spectrum of Cr-doped and -undoped solids calcined at 400°C.

As seen from these absorption spectra, the absorbance bands improved by increasing Cr content in doped samples, which may be attributed to the presence of new electronic states in the band gap of TiO_2 and to the shift of the conduction band edge of Cr-doped TiO_2. Therefore, the band gaps of Cr-doped TiO_2 become slightly smaller than those of undoped TiO_2 [24].

The band gap energies of the samples studied were calculated from these spectra using the Kubelka–Munk function [25]:

$$F(\mathrm{RD}) = \frac{(1-\mathrm{RD})^2}{2\mathrm{RD}} \quad (2)$$

where RD is the diffuse reflectance of solids.

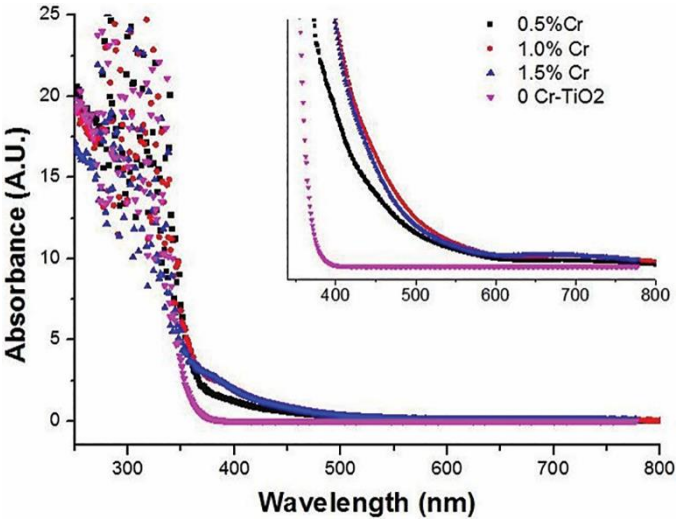

Figure 5 • Absorption spectra. The inset shows the fragment of the absorption spectra in the range of 400 to 800 nm of the doped and undoped solids.

White materials without doping present no absorption within the range of visible light. As shown in the figure, the absorption of materials increases as the chromium concentration increases, which is in line with an increase in the coloration of samples. Band gap (forbidden band) values were determined by extrapolating de linear part of the function: $\left(F(\mathrm{RD})\times E(\lambda)\right)^{0.5}$ vs. $E(\lambda)$.

$$E(\lambda) = \frac{h\times c}{\lambda} \quad (3)$$

where h = Plank constant (eV/s) and c = speed of light (nm/s) [22]. The calculated values decrease as the dopant concentration increases, as can be seen in **Table 4**.

Table 4 • Band gap values, E_g (eV)

Materials	BGap, E_g (eV)
TiO_2-CH	3.27
0.5Cr-TiO_2	3.14
1.0Cr-TiO_2	3.11
1.5Cr-TiO_2	3.01

It is observed that the band gap decreases with increasing dopant concentration, which favors the photocatalytic activity. This behavior, in the doped catalysts, can be attributed to a better adsorption of radiation in the visible light range, due to the oxygen vacancies that occur in the TiO_2 network due to the effect of the substitution of chromium ions on the crystalline network of the titania.

3.5. Nitrogen sorptometry – textural properties

Textural properties of materials are important for photocatalysis. Both specific surface and pore size are relevant for reactants and products to diffuse from and to the material surface so that the photocatalytic process can be successfully carried out. The adsorption–desorption isotherms and the pore size distribution are shown in **Figures 6** and **7**, respectively.

According to the IUPAC classification, all the isotherms of the samples are of classical type IV, typical of mesoporous materials with a H4 hysteresis loop. The surface areas for TiO_2 doped were determined with the BET method. The specific surface values for the doped solids are greater than those for the undoped solid (**Table 5**). Particularly, the highest value was found for 1.0Cr-TiO_2, with pore volume and size being unchanged for all solids. Pore size distribution from 13 to 130 Å can be observed together with uniform distribution of pore canals, which is not affected by dopant concentration [26].

Table 5 • Specific surface, total pore volume, and pore size of the solids

Solids (T = 400°C)	S_{BET} [m²/g]	V_{TP} [cm³/g]	w_p [Å]
0.5Cr-TiO_2	136	0.26	38
1.0Cr-TiO_2	140	0.27	39
1.5 Cr-TiO_2	133	0.26	39
TiO_2-CH	119	0.27	45

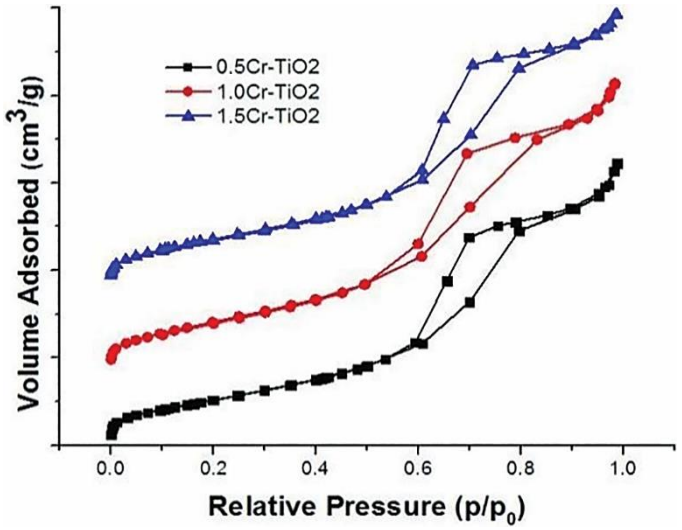

Figure 6 • Adsorption–desorption isotherms for the solids Cr-TiO_2 doped (400°C).

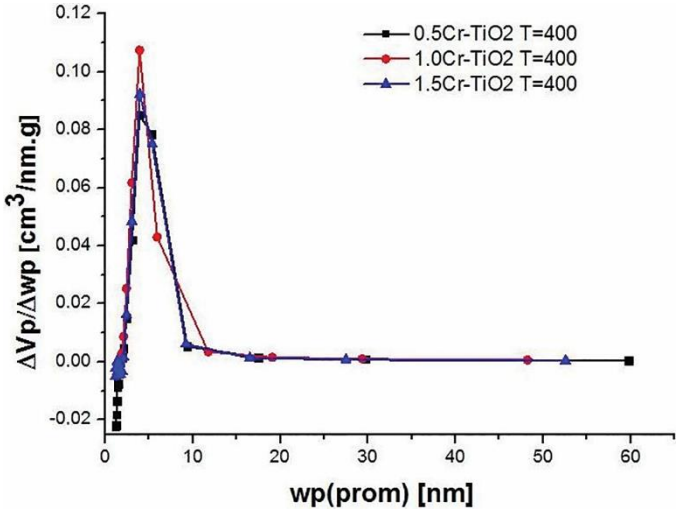

Figure 7 • Pore size distribution for the solid Cr-TiO_2 doped (400°C).

3.6. Zeta potential

One way of assessing the properties of colloidal dispersions is measuring the zeta potential, which depends on the surface charge of particles. **Figure 8** shows the results of zeta potential measurements.

Figure 8 shows that the TiO_2-CH solid shows an isoelectric point or zero charge point (PZC) at pH 6.5, which moves to lower values when adding chromium ions. The PZC of the TiO_2-CH solid matches the value reported in the bibliography for anatase [27–29].

The isoelectric point shift in doped solids toward lower pH values results from the fact that the chromate ion isomorphically replaces titanium in the crystal lattice. This leads to the formation of an extra negative surface charge that requires a higher concentration of protons to be neutralized. The differences in the values of the isoelectric point in doped solids can also be influenced by particle size [30], which depends on the amount of added chromium. Differences can also be influenced by acidic and basic areas on the material surface [31]. However, the presence of the non-predominant polymorphic phase (brookite) has also been reported by other authors who claim that material polymorphisms influence the value of pzc [28]. This leads the values of pzc for brookite to be between 4.7 and 4.9 owing to a more acidic condition of brookite, as opposed to anatase and rutile. Besides, brookite shows a shorter Ti–O bond distance, thus having lower proton affinity. The PZC of doped solids is at 4.6–4.8. It can be concluded that even though the addition of chromium makes the doped solids to have a lower PZC over the range under study, chromium content variation is very low and the differences observed could fall within experimental error.

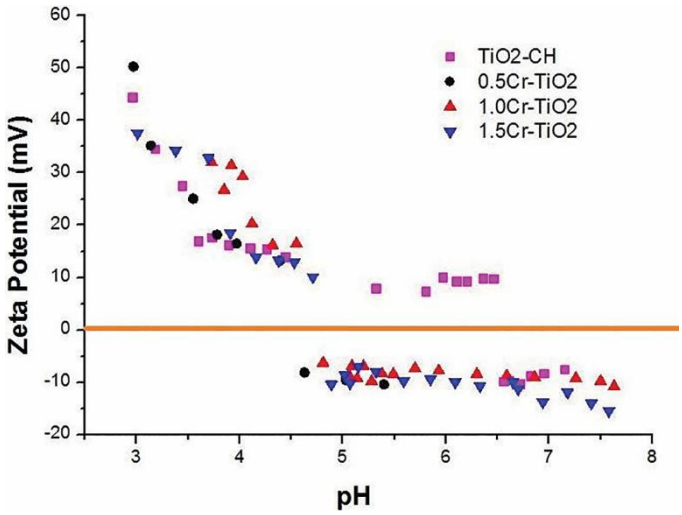

Figure 8 • Zeta potential for doped and undoped solids calcined at 400°C.

3.7. Photocatalytic activities

Photocatalytic activity of solids was studied by monitoring tartrazine degradation. The measurement of the emission spectrum of the lamp used was also carried out, which indicates that these show no lines in the UV light region. The spectrum presents two peaks in the visible light region, at 460 and 650 nm. **Figure 9** shows the spectrum of the lamp used to irradiate the photoreactor.

The removal of the azo dye including absorption in the dark is shown in **Figure 10**. The photocatalytic test of the pure solid (without doping) was carried out, which was observed to slightly increase its concentration (study that will not be included in this work).

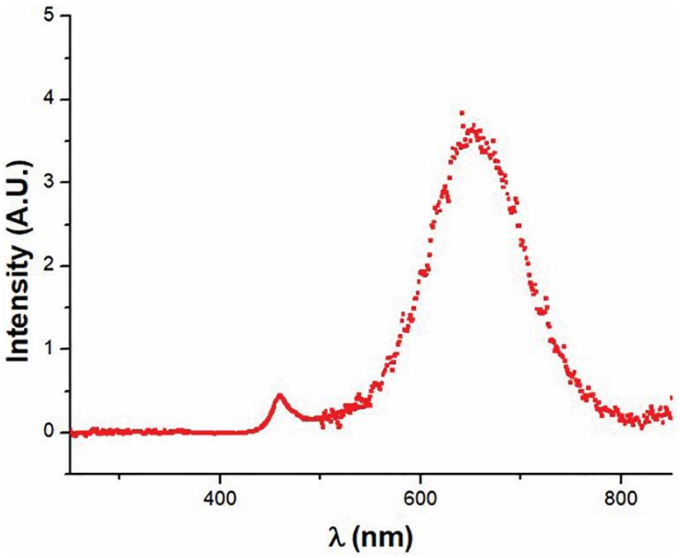

Figure 9 • Emission spectrum of the dichroic LED lamp used.

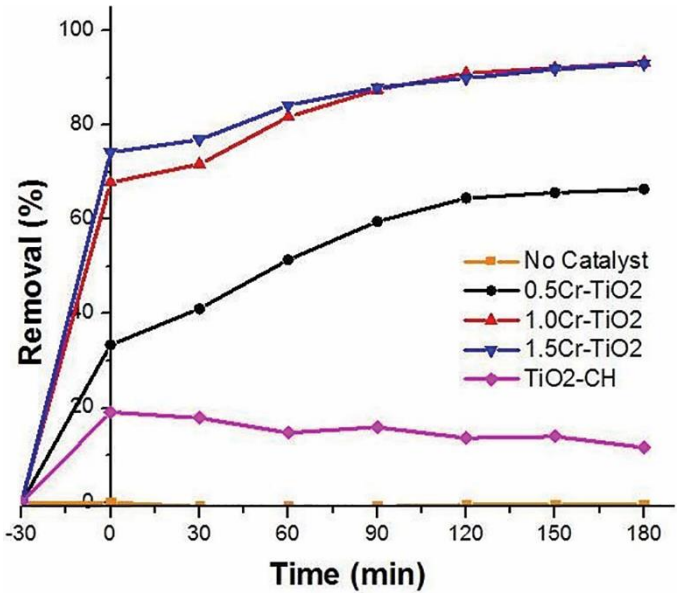

Figure 10 • Tartrazine removal rate for the solids doped and undoped calcined at 400°C.

This increase in concentration is due to a sensitization response of the dye, since it was demonstrated in the absorption spectra that the TiO_2-CH solid is inactive under a visible light source. Sensitization causes degradation of the dye to a greater or lesser extent depending on what percentage of the dye is adsorbed. It is observed that 1.0Cr-TiO_2 and 1.5Cr-TiO_2 solids have similar activity.

It can be observed that the removal rate of the azo dye in aqueous solution catalyzed by the solids calcined at 400°C reaches 93% removal after illumination for 180 minutes.

Likewise, reproducibility and recyclability studies were carried out for the solid with the best performance.

Figure 11 shows that for the first cycle of use the solid reached a degradation percentage of 93%, for the second reuse cycle a 35% and for the third reuse cycle a 21%.

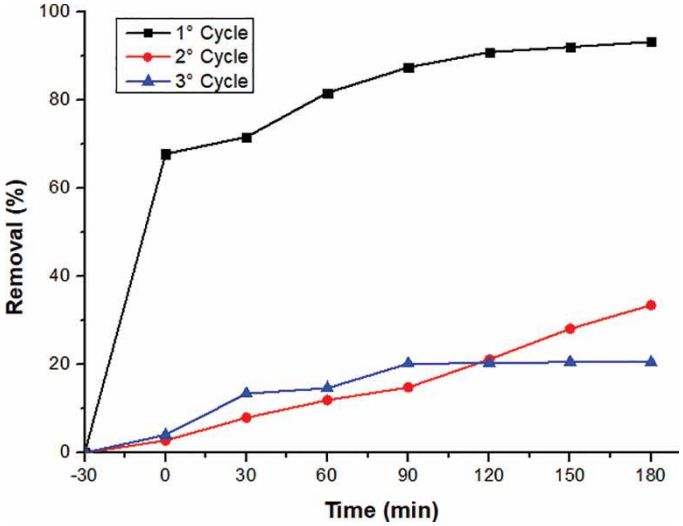

Figure 11 • Reuse cycles of 1Cr-TiO_2 T = 400°C for the degradation of tartrazine.

The actual working catalyst concentrations were 1, 0.5, and 0.22 g/L. It is clearly observed that the degradation decreases with the cycles as well as the catalyst concentration decreases due to the successive sampling and the separation process between cycles.

4. Conclusions

The main purpose of this study was to develop materials capable of reaching photocatalytic degradation under visible light of an azo dye. The synthesis method used here was successfully carried out since it allowed us to obtain chromium-modified titania, photoactive under visible light, by means of a simple and economical synthesis method. Raman spectroscopy and XRD studies allow us to determine the presence of two TiO_2 crystalline phases: anatase and brookite, being the anatase phase the predominant one in all the doped materials. Apart from this, it was determined that as the dopant concentration increases, solids tend to be less crystalline. The studies of optical properties by diffuse reflectance spectroscopy permit us to infer that all synthesized doped solids absorb within the range of visible light, owing to the decrease in the energy value of the forbidden band, due to the presence of new electronic states in the band gap of TiO_2, which in turn could be related to the decrease of the particle size. The studies of nitrogen sorptometry allowed us to determine that the isotherms obtained correspond to type IV, typical of solids with mesoporous structures. The solids present a uniform distribution of pore sizes, which is not affected by dopant concentration within the studied range. Zeta potential studies determined that the zero charge point in doped solids moves toward smaller pH values due to the addition of chromium ions. Photocatalytic activity of solids was studied by means of the degradation of an artificial organic azo dye (tartrazine) under visible light radiation. Even though the solids 1.0Cr-TiO_2 and 1.5Cr-TiO_2 present similar photocatalytic behavior, after 180 minutes of reaction, a degradation average value of 93% was determined for a photocatalyst concentration of 1.0 g/L. This behavior may be attributed to a synergic effect from several events: better radiation adsorption within the range of visible light, owing to oxygen vacancies presumably produced in the TiO_2 lattice, because of the substitution of chromium ions in the titania crystalline lattice, band gap reduction, and a possible decrease in the recombination of the photogenerated charge carriers.

Acknowledgments

The authors wish to thank CIUNSa, INIQUI-CONICET for the financial and logistic support and, in particular, Prof. Víctor Daniel Figueroa (Argentine-British Cultural Association of Salta) for the translation of this article into English.

Funding

This research was funded by the Research Council of the National University of Salta (CIUNSa) and National Council for Scientific and Technical Research (CONICET).

Author contributions

Conceptualization, E.L.S. and E.M.F.T.; methodology, E.L.S. and A.E.C.; software, A.E.C.; validation, E.L.S. and A.E.C.; formal analysis, A.E.C. and G.V.M.; investigation, E.L.S., A.E.C. and G.V.M.; resources, E.L.S., E.M.F.T. and G.V.M.; data curation, A.E.C.; writing—original draft preparation, G.V.M.; writing—review and editing, E.L.S., E.M.F.T. and G.V.M.; visualization, G.V.M.; supervision, E.L.S.; project administration, E.L.S. and E.M.F.T.; funding acquisition, E.L.S. and E.M.F.T. All authors have read and agreed to the published version of the manuscript.

Conflict of interest

The authors declare no conflict of interest.

Data availability statement

Data supporting these findings are available within the article at https://doi.org/10.20935/AcadMatSci6142, or upon request.

Institutional review board statement

Not applicable.

Informed consent statement

Not applicable.

Sample availability

The physical samples used in this study are available in the Materials Laboratory of the Faculty of Engineering of the University of Salta.

Additional information

Received: 2023-09-11

Accepted: 2023-10-15

Published: 2023-12-08

Academia Materials Science papers should be cited as *Academia Materials Science 2023*, ISSN pending, https://doi.org/10.20935/AcadMatSci6142. The journal's official abbreviation is *Acad. Mat. Sci.*

Publisher's note

Copyright

References

1. Hoffmann MR, Martin S, Choi W, Bahnemann D. Environmental applications of semiconductor photocatalysis. Chem Rev. 1995;95:69–96.
2. Karapati S, et al. TiO_2 functionalization for efficient NOx removal in photoactive cement. Appl Surf Sci. 2014;319:29–36.
3. Wang D, Leng Z, Hüben M, Oeser M, Steinauer B. Photocatalytic pavements with epoxy-bonded TiO_2-containing spreading material. Constr Build Mater. 2016;107:44–51.
4. Anpo M. Utilization of TiO_2 photocatalysts in green chemistry. Pure Appl Chem. 2000;72:1265–70.
5. Anpo M. Preparation, characterization, and reactivities of highly functional titanium oxide-based photocatalysts able to operate under UV–visible light irradiation: approaches in realizing high efficiency in the use of visible light. Bull Chem Soc Jpn. 2004;77:1427–42.
6. Grätzel M. Photoelectrochemical cells. Nature. 2001;414:338–44.
7. Hagfeldt A, Graetzel M. Light-induced redox reactions in nanocrystalline systems. Chem Rev. 1995;95:49–68.
8. Shen Q, Arae D, Toyoda T. Photosensitization of nanostructured TiO_2 with CdSe quantum dots: effects of microstructure and electron transport in TiO_2 substrates. J Photochem Photobiol A Chem. 2004;164:75–80.
9. Choi W, Termin A, Hoffmann MR. The role of metal ion dopants in quantum-sized TiO_2: correlation between photoreactivity and charge carrier recombination dynamics. J Phys Chem. 1994;98:13669–79.
10. Usha K, Kumbhakar P, Mondal B. Effect of Ag-doped TiO_2 thin film passive layers on the performance of photo-anodes for dye-sensitized solar cells. Mater Sci Semicond Process. 2016;43:17–24.
11. Zou Z, Wang H, Yang Z. Effect of Au clustering on ferromagnetism in Au doped TiO_2 films: theory and experiments investigation. J Phys Chem Solids. 2017;100:71–7.
12. Yeganeh M, et al. The magnetic characterization of Fe doped TiO_2 semiconducting oxide nanoparticles synthesized by sol–gel method. Physica B Condens Matter. 2017;511:89–98.
13. Jaimy KB, Ghosh S, Sankar S. An aqueous sol–gel synthesis of chromium (III) doped mesoporous titanium dioxide for visible light photocatalysis. Mater Res Bull. 2011;46:914–21.
14. Hamdy MS. One-step synthesis of M-doped TiO_2 nanoparticles inTUD-1 (M-TiO_2-TUD-1, M=Cr or V) and their photocatalytic performance under visible light irradiation. J Mol Catal A Chem. 2014;393:39–46.
15. Tompsett GA, et al. The Raman spectrum of brookite, TiO_2 (Pbca, Z = 8). J Raman Spectrosc. 1995;26:57–62.
16. Granada Ramirez DA, et al. Assessment of Cr doping on TiO_2 thin films deposited by a wet chemical method. Ceram Int. 2023;49:30347–54.
17. Nguyen HH, Gyawali G, Martinez-Oviedo A, Kshetri YK, Lee SW. Physicochemical properties of Cr-doped TiO_2 nanotubes and their application in dye-sensitized solar cells. J Photochem Photobiol A Chem. 2020;397:112514.
18. Bibi S, et al. Cu-doped mesoporous TiO_2 photocatalyst for efficient degradation of organic dye via visible light photocatalysis. Chemosphere. 2023;339:139583.
19. Hou M, et al. Ultrathin carbon-coated Fe-TiO_2-x nanostructures for enhanced photocatalysis under visible-light irradiation. Mater Res Bull. 2023;160:112143.
20. López R, Gómez R, Oros-Ruiz S. Photophysical and photocatalytic properties of TiO_2-Cr sol–gel prepared semiconductors. Catal Today. 2011;166:159–65.
21. Wang C, Shi H, Li Y. Synthesis and characterization of natural zeolite supported Cr-doped TiO_2 photocatalysts. Appl Surf Sci. 2012;258:4328–33.
22. Diaz-Uribe C, Vallejo W, Ramos W. Methylene blue photocatalytic mineralization under visible irradiation on TiO_2 thin films doped with chromium. Appl Surf Sci. 2014;319:121–7.
23. Kernazhitsky L, et al. Photoluminescence of Cr-doped TiO_2 induced by intense UV laser excitation. J Lumin. 2015;166:253–8.
24. Li W. Influence of electronic structures of doped TiO_2 on their photocatalysis. Phys Status Solidi RRL. 2015;9(1):10–27.
25. Makuła P, Pacia M, Macyk W. How to correctly determine the band gap energy of modified semiconductor photocatalysts based on UV–Vis spectra. J Phys Chem Lett. 2018;9(23):6814–7.
26. Fan X, et al. The structural, physical and photocatalytic properties of the mesoporous Cr-doped TiO_2. J Mol Catal A Chem. 2008;284:155–60.
27. Chadwick MD, Goodwin JW, Lawson EJ, Mills PDA, Vincent B. Surface charge properties of colloidal titanium dioxide in ethylene glycol and water. Colloids Surf A Physicochem Eng Asp. 2002;203:229–36.

28. Li H, et al. Hydrothermal synthesis and acidity characterization of TiO_2 polymorphs. Mater Res Bull. 2013;48: 3374–82.

29. He H, et al. Influences of anion concentration and valence on dispersion and aggregation of titanium dioxide nanoparticles in aqueous solutions. J Environ Sci. 2017;54: 135–41.

30. Liu X, Chen G, Su C. Effects of material properties on sedimentation and aggregation of titanium dioxide nanoparticles of anatase and rutile in the aqueous phase. J Colloid Interface Sci. 2011;363(1):84–91.

31. Kosmulski M. Compilation of PZC and IEP of sparingly soluble metal oxides and hydroxides from literature. Adv Colloid and Interface Sci. 2009;152(1):14–25.